WILEY-VCH

FULL PAPER

Design and synthesis of fluorescent-methylphenidate analogues for FRET-based assay of Synapsin III binding

Andrea Casiraghi[a,c]#, Francesca Longhena[b]#, Valentina Straniero[a]*, Gaia Faustini[b], Amy H. Newman[c] §, Arianna Bellucci[b]*§, Ermanno Valoti[a] §

[a] Dr. A. Casiraghi, Dr. V. Straniero, Prof. E. Valoti
Department of Pharmaceutical Sciences
University of Milan
Via Luigi Mangiagalli, 25, 20133, Milano, Italy
E-mail: andrea.casiraghi@unimi.it; valentina.straniero@unimi.it; ermanno.valoti@unimi.it

[b] Dr. F. Longhena, Dr. G. Faustini, Prof. A. Bellucci
Department of Molecular and Translational Medicine
University of Brescia
Viale Europa11, 251223, Brescia, Italy
E-mail: f.longhena@unibs.it; g.faustini004@unibs.it; arianna.bellucci@unibs.it

[c] Dr. A. H. Newman
Molecular Targets and Medications Discovery Branch
NIDA-IRP
333 Cassell Drive, 21224, Baltimore MD, United States
E-mail: anewman@intra.nida.nih.gov

*Correspondence to: valentina.straniero@unimi.it; arianna.bellucci@unibs.it

# These authors contributed equally. § These authors contributed equally

Abstract:

We previously described Synapsin III (Syn III) as a synaptic phosphoprotein that controls dopamine release in cooperation with alpha-synuclein (aSyn). Moreover, we found that in Parkinson's disease (PD), Syn III also participates in alpha-synuclein (aSyn) aggregation and toxicity. Our recent observations point to *threo*-methylphenidate (MPH), a monoamine reuptake inhibitor that efficiently counteracts the freezing gait characteristic of advanced PD, as a ligand for Syn III. Here, we designed and synthesized two different fluorescently-labelled MPH derivatives, one with Rhodamine Red (RHOD) and one with 5-Carboxytetramethylrhodamine (TAMRA), to be used for assessing MPH binding to Syn III by fluorescence resonance energy transfer (FRET). TAMRA-MPH exhibited the ideal characteristics to be used as a FRET acceptor, as it was able to enter into the SK-N-SH cells and could interact specifically with human green fluorescent protein (GFP)-tagged Syn III but not with GFP alone. Moreover, uptake of TAMRA-MPH and co-localization with Syn III was also observed in primary mesencephalic neurons. These findings support that MPH is a Syn III ligand and that TAMRA-conjugated drug molecules may represent valuable tools to study drug-ligand interactions by FRET or to detect Syn III in cytological and histological samples.

Introduction

Parkinson's Disease (PD) is the most common neurodegenerative movement disorder. The available therapeutic options for PD are symptomatic, with no treatments capable of halting or slowing down disease progression[1][2]. The key neuropathological alteration in the PD brain is the loss of dopaminergic neurons in the nigrostriatal system. The resulting reduction of dopamine (DA) in basal ganglia circuits leads to the onset of the classic PD-associated motor symptoms such as rigidity, bradykinesia, tremor and postural instability. Another key histopathological hallmark of the PD brain is the presence of abnormal intraneuronal and intraneuritic insoluble protein aggregates called Lewy Bodies (LB) and Lewy Neurites (LN), respectively. These are mainly composed of α-synuclein (aSyn), a protein enriched at synaptic terminals and governing neurotransmitter release and recycling[3][4][5].

We recently described that the synaptic phosphoprotein Synapsin III (Syn III) interacts and cooperates with aSyn in the control of DA release from mesencephalic neurons[6]. Moreover, we showed that Syn III is another key component of aSyn insoluble fibrils extracted from the post-mortem brains of sporadic PD patients[7] and that Syn III is a crucial mediator of aSyn aggregation and toxicity[8]. Strikingly, our most recent findings suggest that *threo*-methylphenidate (MPH), a monoamine reuptake inhibitor clinically approved for the treatment of attention deficits and hyperactivity disorder (ADHD)[9] and for ameliorating gait freezing in advanced PD[10][11][12][13][14],is able to stimulate an aSyn/Syn III-mediated locomotor response, specifically in aSyn transgenic mice at a pathological stage that exhibit severe dopaminergic functional deficits[15]. This MPH action is lost upon *in vivo* Syn III gene silencing[15], thus suggesting that this protein may act as a target for MPH. Moreover, we observed that MPH does not stimulate locomotion in Syn III knock out mice suggesting these actions are independent of DA transporter inhibition [15].

In this study, we designed, synthesized and tested two different fluorescently-conjugated MPH derivatives to assay their ability to interact with human Syn III by fluorescence resonance energy transfer (FRET) in SK-N-SH neuroblastoma cells overexpressing either green fluorescent protein (GFP) alone (as a negative control) or human GFP-tagged Syn III.
Compounds **1** and **2** (Figure 1) were generated based on a MPH scaffold coupled with two different fluorophores. The choice of the fluorophores was guided by their slightly different excitation/emission spectra, both showing good overlapping with the spectra of the well-established FRET acceptor Red

Fluorescent Protein (RFP). In addition, the different fluorophores are supposed to impart different cell permeability profiles to the assembled probes. The selected fluorophores were connected to the MPH scaffold by two linker chains with distinct chemical properties and comparable length. Specifically, compound **1** featured a Rhodamine Red fluorophore bound to MPH by an amidic alkyl linker (MPH-RHOD), while compound **2** linked MPH to 5-Carboxytetramethylrhodamine (TAMRA) by a PEG4 chain (MPH-TAMRA).

The fluorescence intensity of MPH-RHOD, when excited by the 543 laser, was insufficient to perform FRET studies. However, MPH-TAMRA was found to interact with human green fluorescent protein (GFP)-conjugated Syn III but not with GFP alone in SK-N-SH neuroblastoma cells, as detected by FRET. Moreover, TAMRA-MPH could enter within primary mesencephalic neurons where it co-localized with Syn III-immunopositivity.
These findings support that MPH-TAMRA can enter into cells and can bind Syn III. Moreover, these data provide the first functional design of a fluorescent drug probe to be used to study drug-ligand interaction studies in cells by imaging techniques such as FRET or fluorescence lifetime imaging (FLIM).

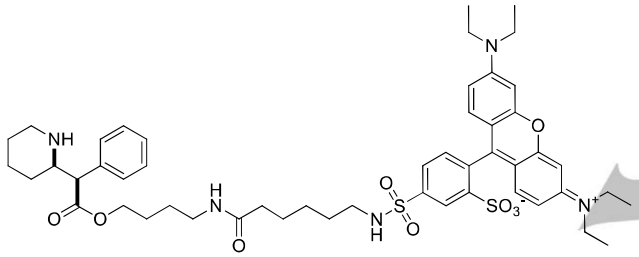

1

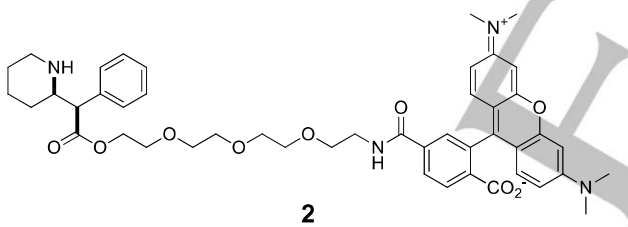

2

Figure 1: Compounds **1** and **2**, object of the present work

Chemistry

The synthesis of **1** and **2** are described in Scheme 1.

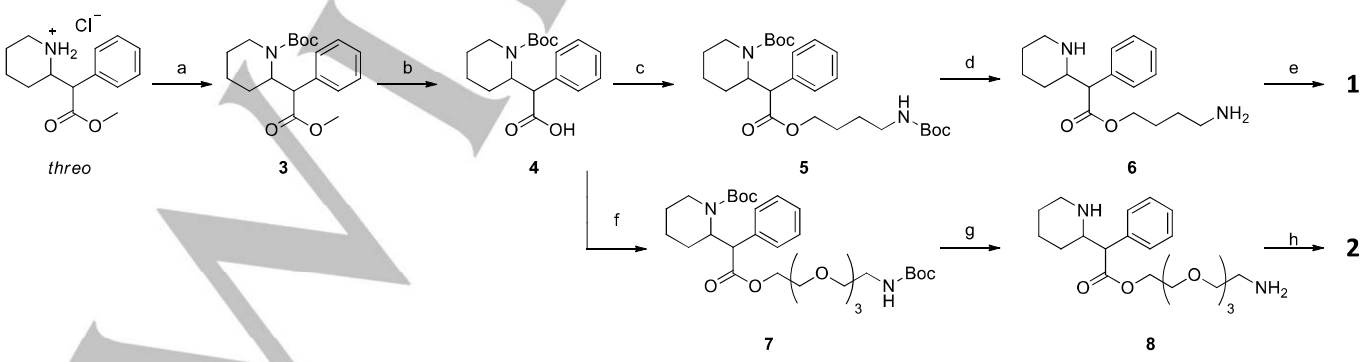

Reagents and conditions: a) Boc_2O, $NaHCO_3$, NaCl, H_2O, $CHCl_3$, reflux (76%); b) NaOH, H_2O, EtOH; c) *N*-Boc-4-aminobutanol, TPP, DIAD, THF, RT (85%); d) 2N HCl/MeOH, RT (65%); e) Rhodamine Red-X NHS ester, DIPEA, DMF, 40°C (98%); f) *N*-Boc-amino-PEG4-alcohol, TPP, DIAD, THF, RT (49%); g) 2N HCl/MeOH, RT (39%); h) 6-COOH-TAMRA, TSTU, DIPEA, RT (12%).

Scheme 1. Synthesis of **1** and **2.**

(*D*,*L*)-*threo*-MPH hydrochloride is first *N*-protected with Boc, to give intermediate **3**, and then hydrolyzed under basic conditions to give *N*-Boc-(*D*,*L*)-*threo*-ritalinic acid **4**.
Compound **4** is the key intermediate of both the final products. In order to obtain **2**, **4** underwent esterification under Mitsunobu reaction conditions with *N*-Boc-4-aminobutanol (**5**) and subsequent deprotection, to give diamine **6**, whose primary amine reacts selectively with commercial Rhodamine Red-X NHS ester to give **1**.

For the synthesis of **2**, the PEG linker is introduced using Mitsunobu reaction conditions with **4** to give *N*-Boc-amino-PEG4-alcohol (**7**). Both the amines of **7** are then deprotected under acidic conditions, to give **8**, which is then reacted with commercial 6-COOH-TAMRA, using a TSTU-based amide coupling protocol. The selective reaction of the NHS ester active intermediate with the primary NH_2 yields **2** as the final compound. Experimental detail and full analytical characterization can be found under the Chemical Synthesis section.

Results and Discussion

Establishment of TAMRA-MPH-Syn III binding by FRET

As a pivotal experiment we first analysed the red fluorescence intensity of SK-N-SH cells overexpressing GFP-Syn III and exposed for 15 min to either RHOD-MPH or TAMRA-MPH. Although the RHOD-MPH-exposed cells were found to exhibit an appreciable red signal when observed by the fluorescence microscope, their exposure to a medium 543 laser intensity was enough to completely quench the red fluorescence signal (Figure 2A). This supported that the fluorescence of RHOD-MPH was not stable enough in the experimental conditions used for the FRET experiments. Given the absence of signal observed, no information on cell permeability and subcellular localization could be obtained for RHOD-MPH. In contrast, the red fluorescence of TAMRA-MPH was intense, even after exposure to a mild 543 laser intensity (Figure 2B). For these reasons, we decided not to employ RHOD-MPH in further experiments and the presented findings are based on TAMRA-MPH.

In order to understand whether MPH is able to bind Syn III we performed acceptor photo-bleaching FRET on SK-N-SH cells transfected with a plasmid transducing GFP-human Syn III after 15 min of either TAMRA or TAMRA-MPH treatment (Figure 3).

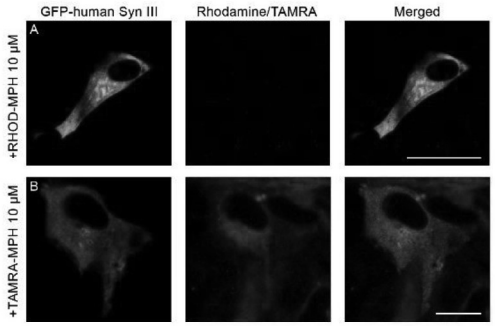

Figure 2: *Representative images showing SK-N-SH cells overexpressing GFP-Syn III and treated with 10 µM RHOD-MPH (A) and 10 µM TAMRA-MPH (B), respectively. As shown in panel (A), RHOD was quenched after 543 laser exposure. Scale bars: 20 µM.*

We evaluated MPH-Syn III binding by measuring FRET efficiency between GFP and TAMRA, since TAMRA shares very similar excitation and emission wavelengths with RFP, a well-established FRET fluorophore when coupled with GFP[16] and we found that, in the presence of increasing concentrations of TAMRA-MPH, FRET efficiency was significantly higher when compared to vehicle-treated cells. Three TAMRA-MPH concentrations (1, 10 and 100 µM) were tested on the basis of our previous findings showing that 10 µM of MPH significantly increases aSyn/Syn III interaction in SK-N-SH cells as detected by FRET[15].

We observed that cells treated with 10 µM TAMRA did not exhibit any red fluorescent signal (Fig. 3B), supporting that the cell permeability of this fluorophore *per se* is very poor. Consistently, these cells did not display differences in the FRET efficiency when compared to control untreated cells (Fig. 3G).

Instead, the cells exposed to increasing concentrations of TAMRA-MPH showed a progressive increase in red fluorescence concentration (Figure 3C-E). Interestingly, we found that, while the cells treated with 1 µM TAMRA-MPH did not exhibit any increase of FRET efficiency when compared to the untreated controls; those exposed to the 10 µM concentration showed a significant (+2.4, $P < 0.001$, One-way ANOVA + Newman-Keuls) increase in the FRET signal (Fig. 3G).

Of note, the FRET efficiency in 100 µM TAMRA-MPH-treated cultures was significantly higher than both untreated (+8.5, $P < 0.001$, One-way ANOVA + Newman-Keuls) and 10 µM TAMRA-MPH treated cells (+6.1, $P < 0.001$, One-way ANOVA + Newman-Keuls), indicating the occurrence of a concentration-dependent increase in MPH-Syn III interaction (Fig. 3G).

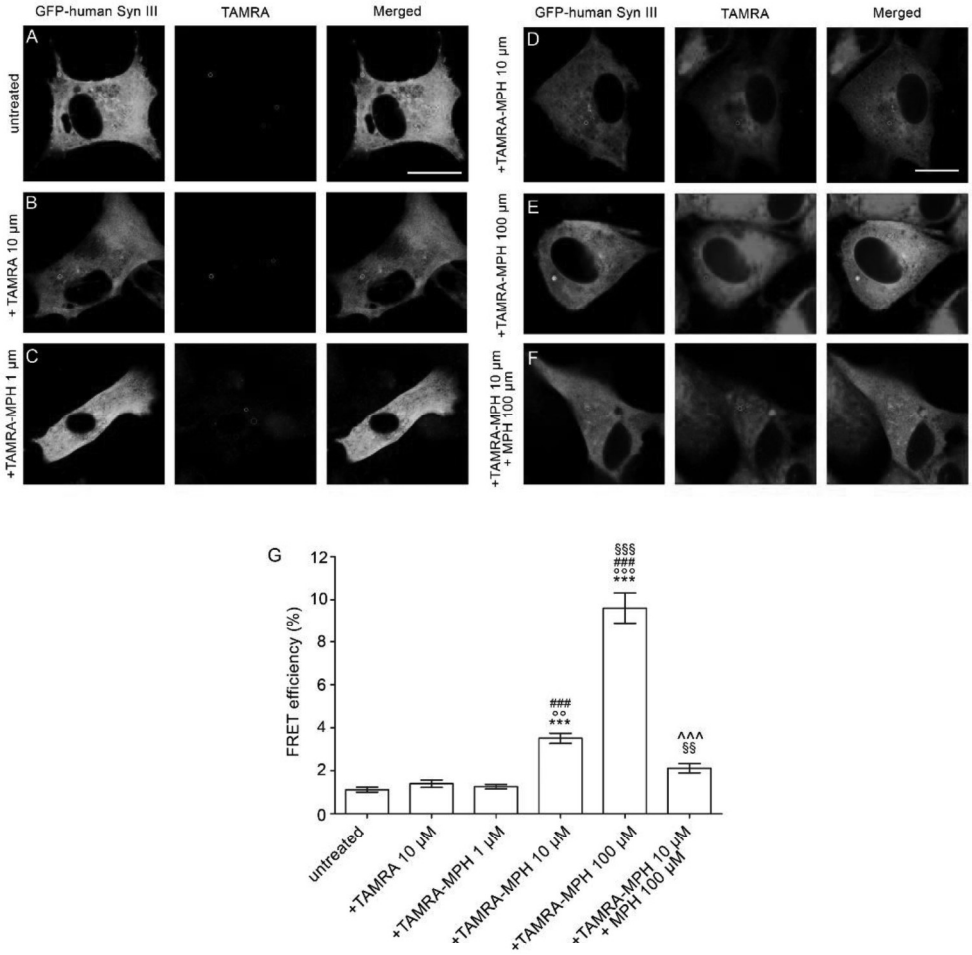

Figure 3: **Images are showing SK-N-SH cells overexpressing GFP-Syn III. Cultures were untreated (A) or treated with either 10 µM TAMRA (B), 1 µM TAMRA-MPH (C), 10 µM TAMRA-MPH (D), 100 µM TAMRA-MPH (E), or 10 µM TAMRA-MPH + 100 µM MPH (F). Scale bars: 20 µm. The histogram (G) summarizes the FRET efficiency in the different experimental conditions (*** P<0.001 vs. untreated; °° P<0.01 vs. TAMRA 10 µM; °°° P<0.001 vs. TAMRA 10 µM; ### P<0.001 vs. TAMRA-MPH 1 µM; §§ P<0.01 vs. TAMRA-MPH 10 µM; §§§ P<0.01 vs. TAMRA-MPH 10 µM; ^^^ P<0.001 vs. TAMRA-MPH 100 µM; One-way ANOVA + Newman-Keuls' post comparison test). The cells treated with TAMRA-MPH exhibited a significant increase of FRET efficiency starting from a concentration of 10 µM, that was inhibited by the presence of MPH 100 µM, as shown**.

To corroborate that TAMRA-MPH binds to Syn III through the MPH moiety, we performed displacement experiments by treating SK-N-SH cells with both 10 µM TAMRA-MPH and 100 µM untagged MPH as binding competitor (Fig. 3F). We observed that the cells exposed to both TAMRA-MPH and untagged MPH exhibited a significant decrease of FRET signal when compared to those exposed to 10 µM TAMRA-MPH alone (Fig. 3G; +1.6, P<0.01; One-way ANOVA + Newman-Keuls). This evidence confirms that MPH binds to Syn III and supports that TAMRA-MPH can be used as a valuable ligand to detect Syn III/MPH interaction by FRET or other imaging methods.

In parallel, we also assessed the ability of TAMRA-MPH to bind to GFP alone as a negative control by using GFP-transfected SK-N-SH cells. In this case, we did not observe differences of FRET efficiency in the vehicle-treated cells when compared to TAMRA-MPH-treated cells (Fig. 4). This finding supports that the FRET signal previously detected in the human GFP-Syn III-expressing cells can be ascribed to TAMRA-MPH/Syn III interaction.

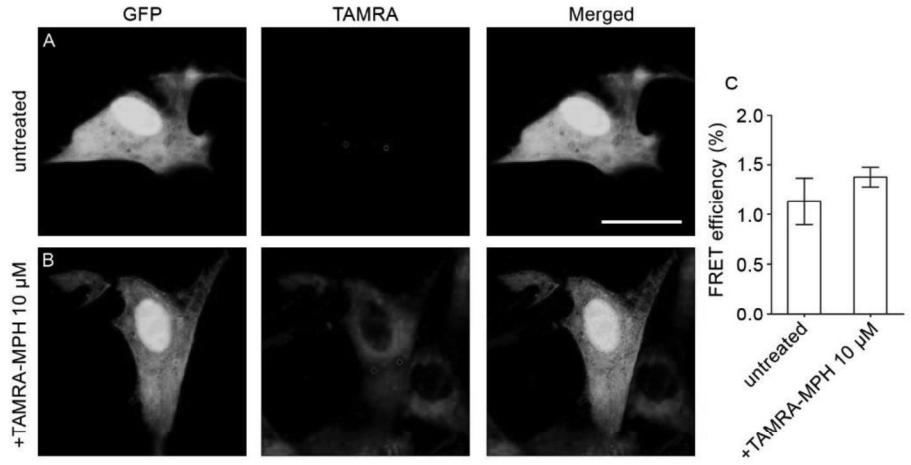

Figure 4: GFP-overexpressing SK-N-SH cells treated with TAMRA-MPH 10 µM (B), respectively. No significant differences in FRET efficiency were detected between untreated cells (A) and cells treated with TAMRA-MPH, as shown in the graph (C) (Student's t-test).

Evaluation of TAMRA-MPH uptake and of its co-localization with Syn III in primary mesencephalic neurons

We then evaluated whether TAMRA-MPH can be internalized by primary cultures of ventral mesencephalic neurons, as in line with the detection of Syn III expression in caudate putamen terminals [17][18][19] , Syn III governs nigrostriatal neurons function[20,21]. In particular, we previously described that exposure of primary mesencephalic neurons to insults inducing aSyn aggregation such as glucose deprivation (GD) induces the formation of aSyn aggregates[21,22] that also result Syn III-immunopositive[21].

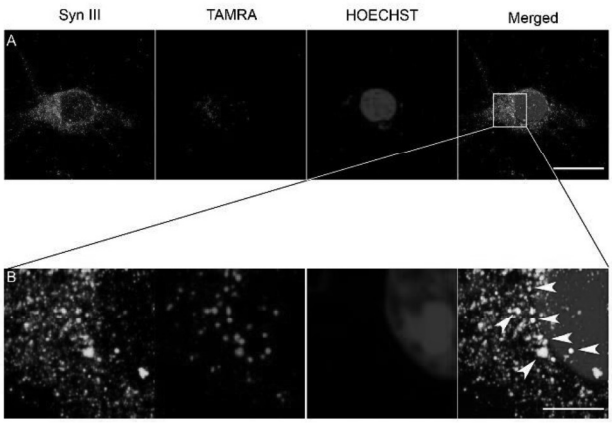

Figure 5: Syn III immunolabeling in primary mesencephalic neurons exposed to GD and treated with 100 nM TAMRA-MPH (A-B). Cell nuclei were counterstained with HOECHST. Note the presence of TAMRA red signal inside the cells in co-localization with the green Syn III-immunopositive signal (arrows in the merge in panel B), supporting the entrance of TAMRA-MPH in neuronal cells and its binding to Syn III. Scale bars: 10 µm (A), 5 µm (B).

Indeed, we observed that GD increases the expression and promotes the compaction of Syn III distribution in this cell culture model[21].

Therefore, this *in vitro* cell system represents an ideal tool to assess the ability of TAMRA-MPH to enter into neuronal cells and to reach Syn III.

Primary mesencephalic neurons were thus exposed to 1 h GD and then subsequently treated with 100 nM TAMRA-MPH for the following 24 hours. Paraformaldehyde (PFA)-fixed cells were the subjected to Syn III immunolabeling and the co-localization of TAMRA-MPH with Syn III immunopositivity was evaluated by Airyscan super-resolution microscopy. We observed that TAMRA-MPH signal exhibited extensive, though not complete co-localization with the Syn III-immunopositive signal (Fig. 5A). In particular, the co-localization appeared more abundant in correspondence of the bigger Syn III-immunopositive dots (Fig. 5B) which are usually indicative of protein aggregates[21].These observations further support for the conclusion that TAMRA-MPH can be internalized by neuronal cells and bind intracellularly to Syn III.

Conclusion

In summary, the present results support that TAMRA owns the ideal GFP-FRET couple characteristics to be exploited for assessing drug-target interactions by this technique. Remarkably, our results indicate that TAMRA-MPH can specifically bind Syn III and can be used to perform FRET-based ligand-receptor interaction studies aimed at deepening our understanding of the pharmacodynamics profile of MPH. In line with our recent observations supporting that Syn III is a key mediator of MPH

action in both physiological and pathological condition[15], the present findings constitute the first evidence demonstrating the ability of MPH to interact with Syn III. Our previous *in silico* studies showed that MPH may also bind to a specific lipid-binding aSyn conformation that is likely generated in advanced stages of PD [23]. Here, we are experimentally showing that Syn III is also a target for MPH, that recognizes Syn III-immunopositive inclusions generated in cells exposed to aSyn pro-aggregating stimuli. Taken together these findings support that TAMRA-MPH could represent a valuable imaging ligand for aSyn/Syn III co-aggregates in PD brains and experimental models of PD. The translational implications of our findings showing the ability of MPH to interact with Syn III surely deserve further investigations. Indeed, we foresee that our observations hold relevant implications not only in the field of PD, but also of ADHD, as this neurodevelopmental disorder has been associated with Syn III polymorphisms[24][25][26] and is routinely treated with MPH.

Experimental Section

Animals

C57BL/6J wild type (wt) mice were used for this study. Mice were bred in our animal house facility at the Department of Molecular and Translational Medicine of University of Brescia, Brescia, Italy. Animals were maintained under a 12-h light–dark cycle at a room temperature (rt) of 22 °C and had ad libitum food and water. All experiments were made in accordance with Directive 2010/63/EU of the European Parliament and of the Council of 22 September 2010 on the protection of animals used. All experimental procedures conformed to the National Research Guide for the Care and Use of Laboratory Animals and were approved by the Animal Research Committees of the University of Brescia (Protocol Permit 719/2015-PR). All achievements were made to minimize animal suffering and to reduce the number of animals used.

Primary mesencephalic neuronal cell cultures and GD

Primary embryonic mouse ventral mesencephalic cells were isolated and cultured as previously described[21]. Briefly, ventral mesencephalic tissues were dissected from C57BL/6J wt mice at embryonic day 13.5. After enzymatic dissociation, the single cell suspension was resuspended in Neurobasal medium (Life Technologies) containing 100 µg/ml penicillin, 100 µg/ml streptomycin (Sigma-Aldrich), 2 mM glutamine (Sigma-Aldrich) and 2% B27 supplement (Life Technologies); cells were then centrifuged, counted and seeded onto poly-D-lysine-coated glass coverslides in 24-well plates for immunocytochemistry (80.000 cells/well), Cells were maintained at 37°C under a humidified atmosphere of 5% CO2 and 95% O2 in Neurobasal medium. After 7 days in vitro, cells were exposed to GD in order to induce aSyn/Syn III aggregation[21,22]. GD was performed through an incubation of the cells with Hank's balanced salt solution (Sigma-Aldrich) supplemented with 2 mM glutamine and 2% of B27 was performed for 1 h at 37°C as previously described[21,22]. After GD the cells were treated with TAMRA-MPH 100 nM for 24 h. N = 3 replicates.

Immunocytochemistry

Twenty-four hours after TAMRA-MPH treatment, cells were fixed by incubating for 15 min in 4% paraformaldehyde with 4% sucrose in 1 M PBS, pH 7.4. Slides were incubated for 1 h at room temperature in blocking solution (2% w/v bovine serum albumin (BSA, Sigma-Aldrich) plus 3% v/v normal goat serum (Sigma-Aldrich) in PBS, then overnight at 4°C with Synapsin III antibody (1:600, Synaptic System). On the following day, cells were incubated for 1 h at room temperature with the 488 fluorochrome-conjugated secondary antibody (Alexa Fluor® 488, Jackson Immunoresearch) diluted in 0.1% Triton X-100 PBS plus BSA 1 mg/ml. After three washes in 0.1% Triton X-100 PBS, cell nuclei were counterstained with Hoechst 33258 dye (Sigma-Aldrich), and the coverslips were mounted onto glass slides using Vectashield (Vector Laboratories, Burlingame, CA).

Confocal microscopy

For acquiring primary neuronal cells images, microscope slides were observed by LSM 880 Zeiss confocal laser microscope equipped with Airyscan super-resolution detector (Carl Zeiss S.p.A.) with the laser set on λ = 405–488–543 nm and z-stack with the height of the sections scanning = 1 µm. Images (512 × 512 pixels) were then reconstructed by Airyscan processing and maximum intensity projection using ZEN Black Imaging Software (Carl Zeiss S.p.A.).

Fluorescence Resonance Energy Transfer (FRET) acceptor photo-bleaching on neuroblastoma cell line

Acceptor photo-bleaching FRET represents a useful method to study protein-protein interaction directly into cells thanks to the application of fluorescent tags [15]. Briefly SK-N-SH cells, a human neuroblastoma cell line that do not express aSyn [27][28], were grown in complete medium composed by Dulbecco's modified Eagle's medium with 1000 mg glucose/l (Life technologies), 10% heat-inactivated fetal bovine serum, 100 µg/ml penicillin, 100 µg/ml streptomycin and 0.01 µM non-essential amino acids (Sigma-Aldrich). Cells were maintained at 37°C under a humidified atmosphere of 5% CO2 and 95% O2. For FRET studies, SK-N-SH cells were seeded onto poli-D-lysine-coated 13 mm glass coverslips in 24-well plates (10000 cells x coverslips) and were maintained in differentiation condition for ten days by daily adding 10 µM retinoic acid to the medium. Seven days after seeding, cells were transiently transfected with plasmids for the expression of Synapsin III tagged with GFP (pGFP-human Syn III) or GFP only (pGFP-empty), by using Lipofectamine 3000 (Life Technologies), according to the manufacturer's instructions. Three days after transfection, cells were treated for 15 min with vehicle (normal saline 0.9%), TAMRA or TAMRA-MPH at different increasing concentrations, then immediately fixed with Immunofix for 15 min and subsequently mounted on glass slides. For displacement experiments the retinoic acid differentiated + Syn III transfected cells were treated for 15 min with both 10 µM TAMRA-MPH and 100 µM untagged *threo*-MPH hydrochloride (Tocris). Once fixed, cells were analyzed by means of a Zeiss confocal laser microscope LSM 880 (Carl Zeiss) with the laser set on λ=488–543. The FRET efficiency (intended as the GFP acceptor recovery after TAMRA acceptor photobleaching) was analyzed by using Zen black (Carl Zeiss). Three-to-six regions of interest (ROI) of each double positive cell were analyzed for 4 series and bleached after the second series with the laser 543 at 65% power. All the FRET value resulting from the different ROI were used for statistical analysis.

Statistical Analysis

Differences between the FRET efficiency of GFP-Syn III overexpressing SK-N-SH cells exposed to TAMRA or different concentrations of TAMRA-MPH were assessed by One-way ANOVA followed by Newman-Keuls multiple comparison test. Differences in terms of FRET efficiency between GFP-overexpressing SK-N-SH cells exposed to TAMRA-MPH or not, were assessed by using Student's t-test. At least N = 15 cells for each experimental condition were analyzed. In each cell 3-6 different ROIs were acquired and the resulting median value for each cell was then plotted and subjected to statistical analysis.

Chemical synthesis

All starting materials were obtained from commercial suppliers and used without further purification. ^{1}H NMR spectra were performed at 400 MHz, using a Varian Mercury Plus 400 instrument; the chemical shifts are reported in ppm. Signal multiplicity is used according to the following abbreviations: s= singlet, d= doublet, dd= doublet of doublets, t = triplet, td= triplet of doublets, q = quadruplet, m = multiplet, sept= septuplet, and

bs= broad singlet. TLC was performed on standard analytical silica gel plates (Analtech Uniplate 250 µm). Chromatographic purifications were performed, in normal phase, using Teledyne ISCO instruments (CombiFlash Rf or CombiFlash EZ) over different RediSep *R*f disposable chromatography cartridges. High Resolution Mass Spectrometry spectra were acquired on LTQ-Orbitrap Velos (Thermo-Scientific, San Jose, CA) coupled with an ESI source in positive ion mode.

ABBREVIATIONS

DCM: dichloromethane; DIAD: diisopropylazadicarboxyate; DIPEA: diisopropylethylamine; DMF: dimethylformamide; mp: melting point; MW: molecular weight; RT: room temperature; THF: tetrahydrofuran; TSTU: *N,N,N',N'*-Tetramethyl-*O*-(*N*-succinimidyl)uronium tetrafluoroborate.

***N*-Boc-*threo*-methylphenidate (3):** *threo* methylphenidate hydrochloride (1.00 g, 3.71 mmol), sodium bicarbonate (716 mg, 8.53 mmol), sodium chloride (867 mg, 14.8 mmol) and Boc_2O (809 mg, 3.71 mmol) were dissolved in a biphasic system of water (5 mL) and chloroform (10 mL) and stirred at reflux for 2.5 hours. The organic phase was separated, washed with 1N HCl (1x5 mL) and evaporated under reduced pressure. The crude product was dissolved in hot hexane (6 mL), stirred at 0° C for 1 hour and filtered to give 0.94 g (76%) of *N*-Boc *threo*-methylphenidate as a white solid. mp: 81.0-84.5° C. ^{1}H NMR (400 MHz, CD_3OD): δ 7.50 – 7.41 (m, 2H), 7.38 – 7.26 (m, 3H), 4.94 – 4.82 (m, 1H), 4.26 (d, *J* = 10.6 Hz, 1H), 4.02 (t, *J* = 13.4 Hz, 1H), 3.60 (s, 3H), 3.18 – 2.98 (m, 1H), 1.74 – 1.59 (m, 2H), 1.51 (s, 9H), 1.41 – 1.28 (m, 2H), 1.26 – 1.16 (m, 2H) ppm.

***N*-Boc-*threo*- ritalinic acid (4):** *N*-Boc *threo*-methylphenidate (330 mg, 1.0 mmol) and NaOH (48 mg, 1.2 mmol) were dissolved in a mixture of water (0.75 mL) and ethanol (0.75 mL) and refluxed for 2.5 hours. The solvents were evaporated under reduced pressure, the residue was taken up in 5% citric acid aqueous solution (1.28 g) and ethyl acetate (1 mL) and stirred at RT for 30 minutes. The aqueous phase was extracted with ethyl acetate (2x1 mL), the collected organic phases were dried over $MgSO_4$ and evaporated under reduced pressure to give 0.25 g (78%) of *N*-Boc *threo*-ritalinic acid as a white waxy solid. ^{1}H NMR (400 MHZ, CD_3OD) δ 7.55 – 7.39 (m, 2H), 7.39 – 7.21 (m, 3H), 4.93 – 4.81 (m, 1H), 4.18 (d, *J* = 11.8 Hz, 1H), 4.10 – 3.92 (m, 1H), 3.19 – 3.01 (m, 1H), 1.72 – 1.59 (m, 2H), 1.50 (s, 9H), 1.42 – 1.30 (m, 2H), 1.29 – 1.08 (m, 2H) ppm.

***N*-Boc-4-aminobutanol:** A solution of Boc_2O (3.67 g, 16.83 mmol) in DCM (15 mL) was added dropwise to a solution of 4-aminobutan-1-ol (1.5 g, 16.83 mmol) and TEA (2.81 mL, 20.20 mmol) in DCM (10 mL). The mixture was stirred at RT overnight. The solvent was evaporated under reduced pressure and rotary evaporation was continued for additional 20 minutes at 90° C. The resulting crude product was purified by filtration on a silica gel plug, eluting at first with hexanes/ethyl acetate 60/40 and then with DCM/MeOH (with 10% 8N NH_4OH) 90/10, to give 1.21 g (38%) of *N*-Boc-4-aminobutanol as a colorless oil. ^{1}H NMR (400 MHz, $CDCl_3$) δ 4.60 (bs, 1H), 3.67 (t, *J* = 5.4 Hz, 2H), 3.20 – 3.10 (m, 2H), 1.65 – 1.53 (m, 4H), 1.44 (s, 9H) ppm.

4-(*N*-Boc-amino)butyl-*N*-Boc-*threo*-phenidate (5): DIAD (92 µL, 0.47 mmol) was added dropwise to a solution of *N*-Boc ritalinic acid (100 mg, 0.31 mmol), *N*-Boc-4-aminobutan-1-ol (89 mg, 0.47 mmol) and triphenylphosphine (123 mg, 0.47 mmol) in THF (5 mL) at 0° C under argon atmosphere. The mixture was kept in the dark and stirred at RT overnight. The solvent was evaporated under reduced pressure and the resulting crude product was purified by flash chromatography on silica gel. Elution with hexanes/ethyl acetate 100/0 to 80/20 gave 130 mg (85%) of 4-(N-Boc-amino)butyl-*N*-Boc-*threo*-phenidate as a colorless oil. ^{1}H NMR (400 MHz, $CDCl_3$) δ 7.44 (d, *J* = 7.1 Hz, 2H), 7.37 – 7.27 (m, 3H), 5.10 – 4.98 (m, 1H), 4.91 – 4.80 (m, 1H), 4.22 – 4.09 (m, 2H), 4.04 – 3.85 (m, 2H), 3.15 – 2.94 (m, 2H), 1.68 – 1.56 (m, 3H), 1.56 – 1.46 (m, 4H), 1.51 (s, 9H), 1.44 (s, 9H), 1.33 – 1.18 (m, 3H) ppm.

***threo*-4-aminobutylphenidate (6**): 4-(*N*-Boc-amino)butyl-*N*-Boc-*threo*-phenidate (0.13 g, 0.26 mmol) was dissolved in excess 2N HCl/MeOH and stirred at RT for 1 hour. 2.0M NH_3 in isopropanol was added dropwise to pH 9 and the solvents were evaporated under reduced pressure and the crude product was purified by flash chromatography on silica gel. Elution with DCM/MeOH (with 10% 8N NH_4OH) 100/0 to 80/20 gave 49 mg (65%) of *threo*-4-aminobutylphenidate as a colorless oil. ^{1}H NMR (400 MHz, $CDCl_3$) δ 7.34 – 7.23 (m, 5H), 4.13 – 4.02 (m, 2H), 3.43 (t, *J* = 5.0 Hz, 1H), 3.13 (dt, *J* = 10.5, 2.5 Hz, 1H), 3.09 – 3.03 (m, 1H), 2.70 (dt, *J* = 11.9, 2.8 Hz, 1H), 2.63 – 2.57 (m, 2H), 1.72 – 1.65 (m, 2H), 1.68 (bs, 3H), 1.62 – 1.53 (m, 2H), 1.45 – 1.31 (m, 3H), 1.31 – 1.16 (m, 2H), 1.02 – 0.88 (m, 1H) ppm.

3,6-bis(dimethylamino)-9-(4-{5[4-(*treo*-2-pyperid-2'-yl-2-phenylacethoxy)buthylaminocarbonyl]penthylaminosulphonyl}-2-sulphophenyl)xanthylium, inner salt (1): A solution of *threo*-4-aminobutylphenidate (1.89 mg, 6 µmol), Rhodamine Red-X NHS ester (5.00 mg, 6 µmol) and DIPEA (1 µL, 6 µmol) in DMF (1 mL) was stirred at 50° C overnight. The solvent was evaporated under reduced pressure and the crude product was purified by flash chromatography on silica gel. Elution with DCM/MeOH (with 10% 8N NH_4OH) 100/0 to 85/15 gave 6.0 mg (98%) of 4-*N*-[6-(Rhodamine Red-4-sulfonamido)hexanoyl]aminobutyl-*threo*-phenidate as a dark purple oil.^{1}H NMR (400 MHz, $CDCl_3$) δ 8.81 (d, *J* = 1.8 Hz, 1H), 8.02 (dd, *J* = 7.9, 1.9 Hz, 1H), 7.30 – 7.20 (m, 9H), 7.03 (t, *J* = 5.6 Hz, 1H), 6.86 – 6.79 (m, 1H), 6.67 (d, *J* = 2.3 Hz, 1H), 4.03 (dt, *J* = 11.9, 6.7 Hz, 1H), 3.92 (dt, *J* = 11.0, 6.6 Hz, 1H), 3.56 (q, *J* = 7.1 Hz, 8H), 3.43 (d, *J* = 10.1 Hz, 1H), 3.11 (t, *J* = 6.6 Hz, 2H), 3.11 – 3.02 (m, 2H), 2.98 (dd, *J* = 12.9, 6.6 Hz, 2H), 2.67 (dt, *J* = 11.7, 2.6 Hz, 1H), 2.06 (t, *J* = 7.5 Hz, 2H), 1.70 – 1.19 (m, 6H), 1.29 (t, *J* = 7.1 Hz, 12H) ppm. HRMS: *m/z* 743.31, 654.22, 559.16.

***N*-Boc-amino-PEG4-alcohol:** A solution of Boc_2O (1.24 g, 5.69 mmol) in EtOH (1 mL) was added dropwise to a solution of amino-PEG4-alcohol (1.00 g, 5.17 mmol) in EtOH (9 mL) under argon atmosphere. The mixture was stirred at RT for 4 hours. DCM (20 mL) was added and the organic phase was washed with 1N HCl (10 mL), saturated $NaHCO_3$ (10 mL) and brine (10 mL). The resulting crude product was purified by filtration on a silica gel plug, eluting at first with hexanes/ethyl acetate 70/30 and then with DCM/MeOH (with 10% 8N NH_4OH) 90/10, to give 1.12 g (74%) of *N*-Boc-amino-PEG4-alcohol as a colorless oil. ^{1}H NMR (400 MHz, $CDCl_3$) δ 5.61 (bs, 1H), 3.77 – 3.68 (m, 4H), 3.68 – 3.59 (m, 8H), 3.55 – 3.51 (m, 2H), 3.36 – 3.27 (m, 2H), 3.01 (bs, 1H), 1.44 (s, 9H) ppm.

[*N*-Boc(amino-PEG4)yl] *N*-Boc-*threo*-phenidate (7): DIAD (0.30 mL, 1.55 mmol) was added dropwise to a solution of *N*-Boc ritalinic acid (0.33 g, 1.03 mmol), *N*-Boc-amino-PEG4-alcohol (0.45 g, 1.55 mmol) and triphenylphosphine (0.41 g, 1.55 mmol) in THF (15 mL) at 0° C under an argon atmosphere. The mixture was kept in the dark and stirred at RT for 24 hours. The solvent was evaporated under reduced pressure and the resulting crude product was purified by flash chromatography on silica gel. Elution with hexanes/ethyl acetate 100/0 to 60/40 gave 0.20 g (49%) of *N,N'*-diBoc-*threo*-ritalinic acid (amino-PEG4)ester as a colorless oil. ^{1}H NMR (400 MHz, $CDCl_3$) δ 7.50 – 7.40 (m, 2H), 7.37 – 7.27 (m, 3H), 5.09 – 4.79 (m, 1H), 4.30 – 4.05 (m, 4), 4.04 – 3.91 (m, 1H), 3.69 – 3.49 (m, 12H), 3.35 – 3.26 (m, 2H), 3.16 – 2.95 (m, 1H), 1.68 – 1.13 (m, 6H), 1.51 (s, 9H), 1.44 (s, 9H) ppm.

(amino-PEG4)yl-*threo*-phenidate (8): *N,N'*-diBoc *threo*-ritalinic acid(amino-PEG4)ester (0.20 g, 0.50 mmol) was dissolved in excess 2N HCl/MeOH and stirred at RT for 1 hour. 2.0M NH_3 in isopropanol was added dropwise until pH 9, the solvents were evaporated under reduced pressure and the obtained crude product was purified by flash chromatography on silica gel. Elution with DCM/MeOH (with 10% 8N NH_4OH) 100/0 to 80/20 gave 0.08 g (39%) of (amino-PEG4)yl-*threo*-phenidate as a colorless oil. ^{1}H NMR (400 MHz, $CDCl_3$) δ 7.31 – 7.21 (m, 5H), 4.30 – 4.23 (m, 1H), 4.17 (dt, *J* = 11.9, 4.6 Hz, 1H), 3.63 – 3.56 (m, 6H), 3.56 – 3.43 (m, 7H), 3.11 (dt, *J* = 10.5, 2.5 Hz, 1H), 3.08 – 3.02 (m, 1H), 2.85 (t, *J* = 5.2 Hz, 2H), 2.67 (dt, *J* = 11.9, 2.8 Hz, 1H), 1.70 – 1.63

(m, 1H), 1.59 – 1.51 (m, 1H), 1.44 – 1.29 (m, 1H), 1.29 – 1.14 (m, 2H), 1.01 – 0.87 (m, 1H) ppm.

3,6-bis(dimethylamino)-9-({5-[*treo*-2-pyperid-2'-yl-2-phenylacethoxy](PEG4)yl aminocarbonyl}-2-carboxyphenyl)xanthylium, inner salt (2): A solution of (amino-PEG4)yl-*threo*-phenidate (4.73 mg, 12 µmol), 6-COOH-TAMRA (5.00 mg, 12 µmol) and DIPEA (2 EQ) (8.4 µL, 24 µmol) in DMF (2 mL) was stirred at RT overnight. The solvent was evaporated under reduced pressure and the obtained crude product was purified by flash chromatography on silica gel. Elution with DCM/MeOH (with 10% 8N NH_4OH) 100/0 to 80/20 gave 1.2 mg (12%) of (Rhodamine Red-4-sulfonyl)amino(PEG4)yl-*threo*-phenidate (Compound XVIII) as a dark purple oil. ^1H NMR (400 MHz, $CDCl_3$) δ 8.10 (s, 1H), 7.64 (s, 1H), 7.35 – 7.20 (m, 7H), 6.66 (d, *J* = 8.9 Hz, 2H), 6.50 (s, 1H), 6.42 (d, *J* = 8.5 Hz, 2H), 4.32- 4.26 (m, 1H), 4.07 – 3.99 (m, 1H), 3.71 – 3.31 (m, 14H), 3.00 (s, 6H), 3.00 (s, 6H), 2.89 – 2.79 (m, 1H), 1.94 – 1.28 (m, 6H) ppm. HRMS: *m/z* 606.29, 588.24, 544.24, 472.15, 456.19, 418.15.

Acknowledgements

This work was supported by the University of Brescia Ex 60% Research Funds to AB and by NIDA Intramural Research Program (Z1A DA000610) during AC's year in the Newman lab. AB is also grateful to the Michael J. Fox Foundation for Parkinson's Research, NY, USA, grant ID: #10742 and #10742.01. We also thank Dr. Ludovic Muller (Structural Biology Core, NIDA-IRP) for high resolution mass spectrometry analyses.

Conflict of interest

The authors declare no conflict of interests, financial or otherwise, in this paper.

Keywords: fluorescent-methylphenidate, TAMRA, FRET, Synapsin III binding, Parkinson's Disease.

References

[1] A. Bellucci, M. Zaltieri, L. Navarria, J. Grigoletto, C. Missale, P. Spano, *Brain research* **2012**, *1476*, 183.

[2] F. Longhena, G. Faustini, M. G. Spillantini, A. Bellucci, *International journal of molecular sciences* **2019**, *20*.

[3] A. Bellucci, N. B. Mercuri, A. Venneri, G. Faustini, F. Longhena, M. Pizzi, C. Missale, P. Spano, *Neuropathology and applied neurobiology* **2016**, *42*, 77.

[4] A. Bellucci, A. Antonini, M. Pizzi, P. Spano, *Frontiers in Aging Neuroscience* **2017**, 330.

[5] L. Calo, M. Wegrzynowicz, J. Santivañez-Perez, M. Grazia Spillantini, *Movement disorders : official journal of the Movement Disorder Society* **2016**, *31*, 169.

[6] M. Zaltieri, J. Grigoletto, F. Longhena, L. Navarria, G. Favero, S. Castrezzati, M. A. Colivicchi, L. Della Corte, R. Rezzani, M. Pizzi et al., *Journal of cell science* **2015**, *128*, 2231.

[7] F. Longhena, G. Faustini, T. Varanita, M. Zaltieri, V. Porrini, I. Tessari, P. L. Poliani, C. Missale, B. Borroni, A. Padovani et al., *Brain pathology (Zurich, Switzerland)* **2018**, *28*, 875.

[8] G. Faustini, F. Longhena, T. Varanita, L. Bubacco, M. Pizzi, C. Missale, F. Benfenati, A. Björklund, P. Spano, A. Bellucci, *Acta neuropathologica* **2018**, *136*, 621.

[9] M. Huss, P. Duhan, P. Gandhi, C.-W. Chen, C. Spannhuth, V. Kumar, *Neuropsychiatric disease and treatment* **2017**, *13*, 1741.

[10] A. Delval, C. Tard, M. Rambour, L. Defebvre, C. Moreau, *Neurophysiologie clinique = Clinical neurophysiology* **2015**, *45*, 305.

[11] C. Moreau, A. Delval, L. Defebvre, K. Dujardin, A. Duhamel, G. Petyt, I. Vuillaume, J.-C. Corvol, C. Brefel-Courbon, F. Ory-Magne et al., *The Lancet Neurology* **2012**, *11*, 589.

[12] D. Devos, P. Krystkowiak, F. Clement, K. Dujardin, O. Cottencin, N. Waucquier, K. Ajebbar, B. Thielemans, M. Kroumova, A. Duhamel et al., *Journal of neurology, neurosurgery, and psychiatry* **2007**, *78*, 470.

[13] N. G. D. Reyes, M. A. C. Bagnas, A. K. D. Antonio, R. D. G. Jamora, *Basal Ganglia* **2018**, *11*, 8.

[14] L. Pollak, Y. Dobronevsky, T. Prohorov, S. Bahunker, J. M. Rabey, *Journal of neural transmission. Supplementum* **2007**, 145.

[15] G. Faustini, F. Longhena, A. Bruno, F. Bono, J. Grigoletto, L. La Via, A. Barbon, A. Casiraghi, V. Straniero, E. Valoti et al., *Neurobiology of disease* **2020**, 104789.

[16] B. T. Bajar, E. S. Wang, S. Zhang, M. Z. Lin, J. Chu, *Sensors (Basel, Switzerland)* **2016**, *16*.

[17] B. Porton, W. C. Wetsel, H.-T. Kao, *Seminars in cell & developmental biology* **2011**, *22*, 416.

[18] I. L. Bogen, J.-L. Boulland, E. Mariussen, M. S. Wright, F. Fonnum, H.-T. Kao, S. I. Walaas, *Journal of neurochemistry* **2006**, *96*, 1458.

[19] V. A. Pieribone, B. Porton, B. Rendon, J. Feng, P. Greengard, H.-T. Kao, *The Journal of comparative neurology* **2002**, *454*, 105.

[20] B. M. Kile, T. S. Guillot, B. J. Venton, W. C. Wetsel, G. J. Augustine, R. M. Wightman, *The Journal of neuroscience : the official journal of the Society for Neuroscience* **2010**, *30*, 9762.

[21] M. Zaltieri, J. Grigoletto, F. Longhena, L. Navarria, G. Favero, S. Castrezzati, M. A. Colivicchi, L. Della Corte, R. Rezzani, M. Pizzi et al., *Journal of cell science* **2015**, *128*, 2231.

[22] A. Bellucci, G. Collo, I. Sarnico, L. Battistin, C. Missale, P. Spano, *Journal of neurochemistry* **2008**, *106*, 560.

[23] G. Faustini, F. Longhena, A. Bruno, F. Bono, J. Grigoletto, L. La Via, A. Barbon, A. Casiraghi, V. Straniero, E. Valoti et al., *Neurobiology of disease* **2020**, *138*, 104789.

[24] Ö. Başay, B. Kabukcu Basay, H. Alacam, O. Ozturk, A. Buber, S. Gorucu Yilmaz, Y. Kıroğlu, M. E. Erdal, H. Herken, *Neuropsychiatric disease and treatment* **2016**, *12*, 1141.

[25] M. Gerlach, M. Sharma, M. Romanos, K.-P. Lesch, S. Walitza, H. A. Conzelmann, R. Krüger, T. J. Renner, *Attention deficit and hyperactivity disorders* **2019**, *11*, 107.

[26] A. N. İ. Kenar, T. Edgünlü, H. Herken, M. E. Erdal, *DNA and cell biology* **2013**, *32*, 430.

[27] L. Navarria, M. Zaltieri, F. Longhena, M. G. Spillantini, C. Missale, P. Spano, A. Bellucci, *Neurochemistry international* **2015**, *85-86*, 14.

[28] Y. Matsuo, T. Kamitani, *PloS one* **2010**, *5*.

Table of Contents

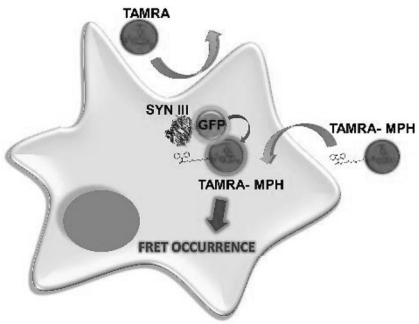

The present study presents TAMRA-*threo*-methylphenidate as a promising tool for the study of drug-ligand interactions.
We designed and synthetized this fluorescent conjugate and we assessed its ability to interact with human Synapsin III, a synaptic partner of alpha-synuclein co-participating in Parkinson's disease pathology, by FRET.